CLM-P 362

CLM-P 362

UKAEA RESEARCH GROUP

Preprint

FUEL-COOLANT INTERACTIONS

Small-scale experiments and theory.

D J BUCHANAN
T A DULLFORCE

CULHAM LABORATORY
Abingdon Berkshire

1973

CLM-P 362

FUEL-COOLANT INTERACTIONS-
SMALL-SCALE EXPERIMENTS AND THEORY

by

D J Buchanan and T A Dullforce

Abstract

The basic physical processes that cause fuel-coolant interactions are being investigated using the techniques of computational physics and analytical theory. Smallscale experiments provide additional support. In this paper some recent experimental and theoretical work is reviewed. It is shown how many of the experimental results can be explained in terms of a recently proposed model. Further consequences of the model are also investigated and it is suggested that there exists a threshold value for the external pressure above which the interaction does not occur.

(Paper to be presented at the Second Specialist Meeting on Sodium Fuel Interaction in Fast Reactors, Ispra, 21st - 23rd November 1973).

UKAEA Research Group
Culham Laboratory
Abingdon
Berkshire

September 1973

dmg

1. Introduction

It is well known that when a hot liquid comes into contact with a cold vaporisable liquid an explosion of considerable violence may occur. This type of explosion is called alternatively a vapour explosion, a thermal interaction or fuel-coolant interaction (FCI), the hot liquid being the fuel and the cold liquid the coolant. These interactions are not the result of chemical change; the energy source is the excess heat in the fuel. FCIs have been observed between cold water and various molten metals (e.g. tin, indium, steel and aluminium), in the nuclear field between molten uranium dioxide (the fuel) and liquid sodium (the coolant), and in the chemical industry between liquefied natural gas, LNG, (the coolant) and water (the fuel). The term 'FCI' has, in the past, been used only of interactions between reactor fuel and reactor coolant but we use it generically to cover all interactions. The interaction between UO_2 and Na has occurred only in very specialized circumstances and there is much interest in determining whether FCIs are physically possible in Na/UO_2 reactors. Witte et al (1970) quote many examples of FCIs. In addition, these authors as well as Brauer et al (1968) and Groenveld (1972) give resumés of some proposed mechanisms for FCIs, however, none of these qualitative descriptions is really satisfactory. Numerous other references may be found in those papers.

Several authors [Katz and Sliepcvich (1971), Katz (1972), Enger et al (1972) and Yang (1973)] have recently discussed a model for the LNG/water interactions based on the theory of homogeneous nucleation (Döring 1973). It is proposed that the water heats the LNG to the superheated, metastable state. The violent explosions occur when the LNG reaches the homogeneous nucleation temperature and sudden vaporisation occurs. However, such a scheme cannot completely account for all FCIs. Firstly, to transfer sufficient energy from fuel to coolant within the observed timescale of the explosion (a few tens of milliseconds for metal/water explosions) an extremely large contact area

between fuel and coolant is needed. Witte et al (1970) have shown that in the case of metal/water explosions heat transfer rates three orders of magnitude greater than those that occur during boiling processes are required. This result implies that the contact area increases by a factor of 10^3. In the case of LNG/water explosions it is just conceivable that the LNG spreads by a sufficient amount (LNG and water have similar densities) but for metal/water explosions no spreading occurs. Secondly, although the homogeneous nucleation temperature of water is about 290^0C, explosions have been observed (Dullforce and Buchanan 1973) between water and tin at an initial temperature below 290^0C. An additional drawback to the superheating model exists in the case of metal/water explosions. Water is notoriously difficult to superheat. For example, experiments with water more than 10 degrees superheated require careful preparation. The water must be boiled for several hours and then kept under vacuum. In industrial explosions, where, of course, the water has not been specially treated, it is unlikely that highly superheated water is produced unless some mechanism in the interaction itself reduces the number of nucleation sites. It must be recognized, however, that it might be possible for water to be transiently superheated to a high degree.

Since FCIs may present a safety problem in the nuclear field as well as in smelting and liquid natural gas industries much theoretical effort has been spent analysing pressure-time histories and the damage that is likely to be caused by a particular history. However, a really adequate treatment of the problem requires that the basic physics of the situation be understood. The aim of the theoretical work at Culham Laboratory is to obtain an adequate model which is capable of describing the complete FCI. We have found it convenient to perform our own small-scale experiments with which the theoretical developments can be compared.

In §2 the experimental work is reviewed and in §3 a recent model for FCI is described. It is shown how many of the experimental results can be explained

by this model. In addition, the model predicts that variation of the external pressure should affect the interaction.

2. Experimental Results

a. Apparatus.

The basic experiment consisted of dropping from a crucible a few ccs. of molten metal into a beaker containing boiled, distilled water. Measurements were made using a thermocouple, an oscilloscope and a high-speed cine camera. The experimental arrangement is shown in Fig 2.1.

In exploratory experiments by McCracken (unpublished) it was found that if the molten metal was coated with oxide then the results were unpredictable, and hence great care was taken to avoid the formation of oxide by either heating the crucible in the reducing part of a calor gas flame or else by heating it electrically in an inert atmosphere of helium. The crucible was tipped manually when the required metal temperature, monitored by a thermocouple, was reached. The distance between the crucible and water surface was as small as possible, about 3 cm., and the water depth was 17 cm. Just above the water surface (typically 0.2 cm) the molten metal interrupted a He-Ne laser beam enabling a voltage pulse from a phototransistor detector circuit to trigger an osilloscope. A microphone was placed outside the glass tank and connected to the oscilloscope to monitor the sound from the interaction, which could also be recorded on 16 mm film. After each experiment the water was replaced by freshly boiled, distilled water (cooled to the desired water temperature) and the debris collected and dried for futher examination.

b. Results.

We define the dwell time and the percentage disintegration (PD) to be respectively the time between the metal first entering the water (i.e. breaking the light beam) and the initiation of the explosive interaction, and the ratio of the mass of fuel comminuted to the original mass. To ascertain the PD, the debris resulting from an interaction was allowed to dry, the large lumps of unexploded fuel separated from the debris, and then the exploded and unexploded

debris weighed separately. The PD was measured both as a function of the initial coolant temperature T_c, and the initial fuel temperature T_f. The results are shown in Fig 2.2 - Fig 2.4; Fig 2.2 displays the dwell time against T_f, Fig 2.3 the PD against T_f, and Fig 2.4 the PD against T_c. These results are preliminary and do not represent a completed experimental programme.

That the PD increases with T_f is to be expected because more energy is available for the interaction at higher temperatures. On three occasions we have observed unusually high PDs at low temperatures, but we are unable to explain these anomolous results. We shall see, in the next section, how the other two curves can be explained. It was found that the PD provided a good criterion for the reproducibility of results; however, the PD is only a good method of judging the violence if it is less than 100%. For example, above 800^{0}C two shots may give a PD of 100% but one may sound more violent and produce much finer debris. Ideally the particle size distribution should be measured but this measurement is not nearly so readily obtained as the PD.

Fig 2.4 confirms the existence of the sharp cut-off which has been found by previous workers (e.g. Brauer et al, 1968; Board et al, 1972). Examination of the debris resulting from interactions at or near the cut-off, shows that explosions have occured from within lumps of fuel (plate 1) and that the fuel has indentations which suggests that it may have been penetrated by high-velocity jets of liquid coolant (plate 2).

Cine film shows that after entering the water the metal blob, falling under gravity, alters shape, particularly at the front end which tends to flatten. Some air entrained upon entry breaks away and rises towards the water surface. After the dwell time the interaction starts and proceeds as a series of cycles. Each cycle, or explosion, produces a vapour bubble which expands, shredding and dispersing the fuel. When the bubble collapses it is followed by a more violent explosion and the growth of a larger vapour bubble, and so on for three or four oscillations. This series of interactions was also found by Board et al (1972). Pressure waves deform the water surface and, in principle, this could enable the theory of underwater explosions to be used in

calculating the initial pressure for the first explosion. However, this entails that the shape of the deformed surface and its velocity at one point be measured; these measurements are certain to be subject to large errors.

We have not performed any carefully controlled experiments in which the effect of noncondensible gas is investigated. McCracken's preliminary experiments indicate that noncondensible gas, carbon dioxide, dissolved in the coolant has a damping effect but R C Asher, AERE, has found that dissolved oxygen has little effect. It should be noted, however, that the solubility of CO_2 in water is 30 times that of O_2.

3. A Model for FCI

The experimental results presented in the previous section suggest the following model. The interaction is divided into five stages, the last four of which occur cyclically.

Stage 1: as a result of some triggering mechanism (for example, the onset of transition boiling as the hot liquid cools) the liquids come into intimate contact and a vapour bubble is formed.

Stage 2: the vapour bubble expands and then collapses as a result of condensation in the subcooled coolant. Because of the density and/or viscosity difference between fuel and coolant (and also possibly because a solid crust has formed on the fuel) the bubble collapse is asymmetric and a high velocity jet of liquid coolant, directed towards the fuel, is formed.

Stage 3: The jet of liquid coolant penetrates the fuel and, since it has a high velocity, its subsequent disintegration and hence increase in fuel coolant contact area is extremely rapid.

Stage 4: as the jet of coolant penetrates and breaks up heat is transferred from the surrounding fuel to the jet and since the surface area is increasing rapidly the total heating rate also increases rapidly.

Stage 5: when the jet has been heated to a certain temperature it suddenly vaporizes and a high pressure vapour bubble forms. The rapid expansion of this bubble disperses the surrounding fuel into the coolant in an analogous manner to the spray of water produced by a depth charge. The process now proceeds from stage 2 again.

Because of the cyclic scheme some of the energy released from the fuel during each cycle is fed into subsequent cycles and it is this feedback that enables a small initial perturbation to grow. Note that the model provides a mechanism for increasing the contact area between fuel and coolant which is essential to explain the observed rapid heat transfer.

Under certain conditions the second and subsequent cycles may be weaker than the preceeding ones and in these conditions the initial perturbation (stage 1) is stable and does not lead to an explosion. However, under other conditions subsequent cycles are more energetic than the preceeding ones and in this case an explosion occurs.

Similar models involving feedback have been considered by other authors [Potter and Jakeman (1972 a,b); Roberts (1972); Board et al (1972)] but no detailed calculations have been performed. Peckover and Roberts (see Roberts 1972) have developed a simple model in which part of the energy released as each new element of surface is created goes into the turbulent velocity field, which in turn creates new surface. They find that the energy released is infinite at some finite time. However, Peckover and Roberts recognize that their model proposes no mechanism for the feedback. In the model discussed here the feedback mechanism is discussed.

We now give a fuller account of each stage, and, in particular, stage 1 since many of the experimental results can be interpreted in terms of the trigger mechanism. Detailed descriptions of stages 2 - 5 have been given elsewhere (Buchanan and Dullforce 1973, Buchanan 1973a).

Stage 1:

Experiment has shown that the interaction can be triggered in a number of seemingly different ways. Two examples are: (a) the automatic triggering if the coolant temperature is below the threshold, and (b) a mechanical disturbance as found by Board et al (1972). We therefore regard stage 1 solely as a means of supplying the initial perturbation which causes the first bubble to form adjacent to the fuel surface.

Witte et al (1970) have summarised the violent boiling theory of FCI. This theory asserts that if the fuel enters the transition boiling regime (Fig 3.1) then violent boiling tears the fuel apart and causes an FCI.

We do not believe that the onset of transition boiling is the complete cause, rather that it is a means of supplying the initial perturbation required by stage 1. This view is also held by Board et al (1972). The boiling curve can however, be used to explain the results of Figs 2.2 and 2.4 as follows.

Suppose some critical heat flux Q_c is required before the initial bubble can form (Fig 3.2). (The reason for not locating Q_c at the trough of the boiling curve will shortly become apparent.)

Q_c corresponds to some temperature T_T and so the existence of the dwell time is explained simply as the time required for the fuel surface temperature to fall from its initial value, T_f, to T_T. The shape of the dwell time curve also follows from the boiling curve. If the heat flux from the surface at temperature T is proportional to T^α and the rate of cooling is proportional to the heat flux (i.e. $\dot{T} \propto -T^\alpha$) then the time t_T taken to cool from T_f to T_T increases as shown in Fig 3.3 (see also the appendix).

Note that the t_T/T_f curve is concave upwards if $\alpha < 0$, concave downwards if $\alpha > 0$, and linear if $\alpha = 0$. If $\alpha < 0$ then the rate of cooling decreases as T_f is increased and this is also the case in the transition boiling regime. Thus if Q_c is at the location shown in Fig 3.2 then the dwell time curve will be concave upwards for $T_f < T_{min}$. The experimental dwell time curve is concave upwards, hence both the existence and the shape of the dwell

time curve are explained by having Q_c at the location shown. If $T_f > T_{min}$ then the rate of cooling initially decreases as cooling occurs and then increases when T_{min} is passed. In the radiation dominated region $\alpha = 4$ and so t_T reaches a finite limit as T_f is increased indefinitely. The complete dwell time curve is shown in Fig 3.4. Clearly further experiments are required at higher values of T_f to test these ideas.

The cut-off coolant temperature can be explained in two different ways. As the subcooling is decreased, i.e. the coolant temperature increased, the boiling curve moves to the left and the maximum is lowered (Farahat 1972). Hence, either (a) Q_c is not attained (Fig 3.5) or (b) when Q_c is attained the fuel has solidified (Fig 3.6). The second explanation has been suggested by a number of previous authors e.g. Witte et al (1970) implicitly attribute it to Swift (1965). In both cases the dwell time for a given T_f ought to increase as the subcooling is decreased. Board et al (1972) have precipitated an interaction above the cut-off temperature by disturbing the system with a pressure pulse which is propagated several seconds after the initial contact of fuel and coolant. The accepted explanation is that the pulse collapes the vapour layer causing enhanced heat transfer, thus Q_c can be attained. This experiment seems to support (a) above and refute (b).

A second parameter that affects the location of the boiling curve is the ambient pressure. As the pressure is increased the boiling curve moves to the left and the maximum is raised; further increase in the pressure results in the decrease of the maximum as the curve continues to move to the left (Chichelli and Bonilla 1945, Farber and Scorah 1948, Hesse 1973). Therefore, if either of the boiling curve explanations of triggering is correct, there exists a threshold in the ambient pressure above which the interaction does not automatically proceed. Nevertheless, even above this threshold a pressure pulse should still trigger the interaction by collapsing the vapour layer.

A large proportion of the arguments advanced in this section depend on the boiling curve. Nearly all experimental boiling curves are determined

under quasi-static conditions but an FCI is a transient effect and often occurs in the presence of a fluid velocity field. The determination of the boiling curve under these conditions will be necessary before any qualitative conclusions can be drawn from stage 1. Walford (1969) has made some progress in this direction.

Stage 2:

All our calculations henceforth will start with the assumption that an initial bubble has been formed in stage 1. A detailed exposition can be found in Buchanan (1973a).

We assume that the initial condition for the i^{th} cycle is a spherical bubble, initial pressure P_i and radius R_i, which expands in the surrounding incompressible coolant of density ρ_c and ambient pressure P_o ($P_i > P_o$). We assume that the bubble expands until the maximum radius is reached and that during this expansion phase no heat transfer occurs and hence that the mass of vapour in the bubble is constant. When the maximum radius is reached we assume that all the vapour suddenly condenses due to the surrounding sub-cooled liquid. A cavity now exists in the coolant and this cavity collapses under the external pressure P_o. Clearly this is an idealised description of this stage - heat transfer does occur during the expansion phase; however, the simple assumptions made here result in an elementary calculation and since, at this stage, we seek only to postulate a possible mechanism the refined calculation is not necessary.

By using the Rayleigh equation the maximum radius R_m, and the time to expand are easily found. The expansion and collapse of the bubble takes place adjacent to the fuel surface. It is well known that when an initially spherical cavity collapses adjacent to a solid wall the collapse is axi-aymmetric and a jet of liquid, directed towards the wall, is produced. Plesset and Chapman (1971) have done a numerical simulation of this situation and they find that the final jet velocity scales as $(\Delta P/\rho_c)^{\frac{1}{2}}$ where ΔP ($= P_o$ in this case) is the pressure difference causing the collapse.

The final jet dimensions scale as the initial (pre-collapse) cavity radius. Thus the jet dimensions are determined by R_m and consequently by R_i and P_i. The velocity, length and diameter of the jet when it strikes the fuel are

$$V_o = V_c\left(\frac{\Delta P}{\rho_c}\right)^{\frac{1}{2}}$$

$$L_o = L_c \; R_m$$

$$d_o = d_c \; R_m$$

The phenomenon of jetting is due to the lack of spherical symmetry in the local surroundings and thus the constants V_c, L_c and d_c are determined by the degree of departure from spherical symmetry. For bubble collapse adjacent to a solid wall $V_c = 13.0$, $L_c = 0.493$, $d_c = 0.237$.

If the adjacent layer of fuel is liquid than the collapse will still be axi-symmetric (due to the density difference and/or viscosity difference) but the numerical values of the constants will be different. The time to collapse is of order $R_m\sqrt{\frac{\rho_c}{P_o}}$.

Stage 3:

The jet of coolant (diameter d_o and length L_o) enters the fuel with velocity V_o. [A solid crust may exist on the fuel surface but Buchanan (1973b) has shown that provided the bubble radius prior to collapse is greater than a certain minimum size then penetration will still occur]. Christiansen and Reynolds (1971) have done a numerical simulation of this situation using the computer code VORTEX [Christiansen (1970)]. They show that the length of the jet (the calculation is two-dimensional) increases exponentially with a time constant proportional to d_o/V_o. Fig 3.7 illustrates their results

$$L = L_o \; e^{t/\tau}$$

where

$$\tau = f \; d_o/V_o$$

(t is measured from the time the jet starts to penetrate the fuel). Christiansen and Reynolds' results indicate that f has the value 11/8,

however, VORTEX can only handle fluids of equal density and so f will have a different value from that above since fuel and coolant have different densities. Taylor's (1963) results suggest that $f = \frac{11}{8}\left(\frac{\rho_f}{\rho_c}\right)^{\frac{1}{2}}$ where ρ_f is the density of the fuel. Peckover (1971) has explained Christiansen and Reynolds' results by showing that the local vorticity increases exponentially. Batchelor (1952) has investigated the effect of homogeneous turbulence on material lines and surfaces, and he also finds that the length of a line increases exponentially. In addition, he has shown that the area of a material surface increases exponentially with a time constant double that for the length increase. Thus we assume that the surface area of contact between the fuel and the jet is given by

$$A = A_o \, e^{t/\tau}$$

$$\tau = \frac{11}{4}\left(\frac{\rho_f}{\rho_c}\right)^{\frac{1}{2}} \frac{d_o}{V_o}$$

A_o is the initial surface area of the jet. Whilst the jet remains liquid its volume is almost constant. Consequently, since the area increases exponentially the average distance, s, between material surfaces must decrease exponentially.

There are three factors limiting the area increase. Firstly, if the fuel surrounding the jet solidifies then no further increase in contact area can occur. Secondly, if the jet vaporizes then the conditions are radically altered. A high pressure bubble now exists and this blows out the surrounding fuel. Thirdly, the minimum distance between surfaces may be determined by a critical Weber number [Hinze (1948)]. In this case surface tension limits the value of s. We denote the minimum value of s by s_m.

Stage 4:

As the jet penetrates the fuel heat transfer occurs. Fig 3.8 represents a cross-sectional view of the situation sometime after the initial impact. We assume that heat transfer takes place one-dimensionally across each element

of fuel-coolant-fuel as shown in Figs 3.8 and 3.9 .

The thickness of the element of coolant, s(t), is a decreasing function of time until the minimum size s_m is attained. Thereafter, the thickness is constant. Buchanan (1973c)has discussed a variety of methods of treating the problem of heat transfer across a hot-wall/liquid interface. In the ODE method described in that paper it is assumed that the temperature and pressure are uniform within some region of the coolant. It follows that T, the temperature of the coolant, is given by

$$c\rho_c \times x \frac{dT}{dt} = r_1 - r_2 T$$

r_1 and r_2 are parameters specifying the rates of heating and cooling per unit area and x is given essentially by s(t). c is the coolant specific heat. For the successive values of x this equation is easily solved for T.

Stage 5:

When the jet of coolant has been heated to its saturation temperature T_{sat}, it, the jet, vaporizes provided nucleation sites are available (heterogeneous nucleation). An estimate of the time required to supply the latent heat can be made using the latent heat equivalent temperature $\Delta T_L = L/c$, where L is the latent heat of vaporization of the coolant. The time required to heat the coolant to a temperature ΔT_L above T_{sat} is an estimate of the time to supply the latent heat. If no nucleation sites are available the jet must be heated to the homogeneous nucleation temperature before vaporization occurs. For water the homogeneous nucleation temperature, T_{hn}, is about 290^0C. When the jet starts to vaporize by this process the rate of vaporization is so rapid [$\sim 10^{-6}$sec, Rodebush (1952)] that the latent heat cannot be supplied by normal heat transfer from the surrounding fuel. Instead the heat is supplied by the jet itself. If m_v and M_j are respectively the masses of vapour formed and the jet itself then β ($= m_v/M_j$) has the values 0.33 (homogeneous nucleation) and unity (heterogeneous nucleation) (Buchanan 1973a). Since a finite mass of liquid is vaporized virtually

instantaneously the initial state after vaporization is a high-pressure, high-density gas bubble which expands and sends out a shock wave. The pressure at any point in the liquid, distance r from the centre of the bubble, can be calculated as function of time by using weak shock wave theory (Cole 1965) and, although the initial pressure in the bubble is high, the Rayleigh equation may be used to calculate its motion. Thus the vapour bubble is described by stage 2.

Results

The model predicts a series of pressure pulses at the point r (Fig 3.10). Buchanan (1973a) has shown that the ratio of successive peak pressures is

$$\frac{P_i\,(r) - P_o}{P_{i-1}(r) - P_o} = \left(\frac{3}{16}\ \beta\ d_c^{\,2}\ L_c\ \frac{\rho_c}{\rho_\ell} \right)^{1/3} (1+z_r)$$

which for an external pressure of 1 bar gives

$$\frac{P_i\,(r) - P_o}{P_{i-1}(r) - P_o} = \begin{cases} 6.673; & \text{(heterogeneous nucleation)} \\ 2.899; & \text{(homogeneous nucleation)} \end{cases}$$

Z_r is determined by P_i and P_o. The ratio of successive pressure peaks becomes unity at a value of the external pressure, P_{th}, satisfying

$$P_{th} = \frac{3\alpha^3}{1+\alpha+\alpha^2}\ P_i$$

where $\alpha^3 = \frac{3}{16}\ \beta\ d_c^{\,2}\ L_c\ \frac{\rho_c}{\rho_\ell}$. This equation is implicit since P_i and β depend on the external pressure. We find

$$P_{th} = \begin{cases} 67.5 \text{ bar} ; & \text{(heterogeneous nucleation)} \\ 13.0 \text{ bar} ; & \text{(homogeneous nucleation)} \end{cases}$$

If the external pressure is greater than P_{th} then any initial perturbation is damped out.

The total mass of heated coolant, M_c, is also easily shown to be

$$M_c = \frac{\pi}{4} \rho_c \, d_c^2 \, L_c \, \frac{\xi^N - 1}{\xi - 1} \, R_{m_1}^3$$

where $\xi = \alpha^3 \, (1+z_r)^3$ and R_{m_1} is the radius just prior to collapse of the initial perturbing bubble. The ratio of the kinetic energy of the jet just as it starts to penetrate, E_j, to the energy of the bubble, E_b, calculated as the work done by the bubble expanding to its maximum radius, is independent of cycle number and is given by

$$\frac{E_j}{E_b} = \frac{3}{32} \, d_c^2 \, L_c \, V_c^2$$

$$\text{i.e. } E_j/E_b = 0.439$$

An essential feature of the above results is their dependence on V_c, L_c and d_c. The values quoted for these constants are for an empty cavity collapsing adjacent to a solid wall. The effect of gas in the cavity is to reduce the amount of jetting, thus L_c and d_c decrease and this affects the interaction dramatically. For example, if L_c and d_c are reduced to half of their present values the threshold pressure is reduced by a factor of order 1/8, the ratio of successive pressure peaks is half the present value and thus after five cycles the pressure is only 1/32 of its present value. Clearly the determination of V_c, L_c and d_c under a variety of conditions is required.

The analytical results expressed above provide useful checks on the computer code that has been written to solve the model equations. The results of the computations are presented in Figs 3.11 - 3.16 and Tables 3.1 - 3.3 . All the calculations are started with a cavity of radius 10^{-4}m. The cavity collapses and the interaction proceeds. The heterogeneous nucleation process is used for vaporization. Table 3.1 shows how an initially small perturbation can produce large amounts of energy in just a few cycles. E(i) is the work done by the bubble expanding during the i^{th} cycle. T(i) is the time taken to complete i cycles. $P_i(r)$ and $I_i(r)$ are the peak pressure and impulse due to the i^{th} cycle at a point r from the interaction. In all these calculations

r is 10 cm. Figs 3.11 - 3.15 show the effect of varying the external pressure. It may be seen that even an increase of a few bars in pressure has a dramatic damping effect on the interaction. Tables 3.2 and 3.3 and Fig 3.16 show the effects of varying r_1, r_2 and s_m. Initially as r_1 is increased only the time is altered but as r_1 is increased further the energy $E(i)$ is reduced. At such large values of r_1 the heating rate is so great that not all the jet is vaporized, (the maximum observed laboratory heat transfer rates are of the order 10^7 Jm^{-2} s^{-1}.) An increase in r_1 represents an increase in the efficiency of energy transfer and hence the interaction time is reduced, but because it is the product $r_1 A$ that gives the <u>total</u> heating rate and A is exponentially increasing, the interaction time is only slightly altered for large changes in r_1. Variation of r_2 affects the time slightly. Fig 3.16 shows the effect of s_m. For small values of s_m the time for the interaction is independent of s_m since the jet is vaporized before s_m is attained, however, as s_m increases the time for the interaction increases since the minimum size is reached before vaporization occurs.

4. Conclusions

One of the principal difficulties in obtaining useful experimental results on FCI is that no good standard method of calibrating an explosion has been adopted. However, it has been found at Culham that the PD provides a useful means of comparing interactions which occur under different initial conditions. By using PD as a measure the reproducibility of results may also be easily checked.

A large number of small-scale metal-water interactions have been performed and classified according to their PD and initial conditions. Plots of PD against the initial coolant and fuel temperatures show that a cut-off coolant temperature exists and that the violence of the interaction increases as the initial fuel temperature increases. In addition, the dwell time that elapses before an interaction starts has been measured as a function of the initial fuel temperature. The experimental work has led to the proposal of a model

for FCI. The interaction is divided into five stages the last four of which occur cyclically. Many of the experimental results can be explained by the first stage of the interaction; the remaining four stages provide a feedback mechanism by which large quantities of energy are released in a short time from a small initial perturbation. The efficiency of this feedback is reduced as the external pressure is increased; indeed there exists a threshold value for the pressure above which any initial perturbation is damped out.

In the reactor situation, if the containment is sufficiently good it may be that an FCI in part of the reactor will not trigger FCIs in other parts of the reactor because the high pressure resulting from the original FCI is sustained and thus interactions elsewhere are suppressed. That is, FCIs are self-limiting if the resulting pressure is maintained.

The effect of noncondensible gas is not included specifically in the model, nevertheless, as we have pointed out, its presence within the vapour bubbles can be taken into account via the constants V_c, L_c and d_c. Pockets of non-condensible gas throughout either the fuel or coolant or both will tend to cushion any high pressures, thus we would expect that the interaction is damped in the presence of noncondensible gas.

Acknowledgements

Valuable discussions with many collegues too numerous to name are acknowledged. We are particularly grateful to J A Reynolds. This work was done under UKAEA, Risley Intergroup Requisition No. F 214. The support of SRD at UKAEA, Culcheth is also acknowledged. Mr B Jones gave valuable assistance with the experimental work.

APPENDIX

If the heat flux is proportional to T^{α} and the rate of cooling proportional to the heat flux then

$$\frac{dT}{dt} = - kT^{\alpha} \qquad (1)$$

We wish to find t_T, the time to cool from T_f to T_t, as a function of T_f and α . The solutions of eqn. (1) for various α can be written as

a. $\alpha > 1$

$$t_T = \frac{1}{k(\alpha-1)} \left\{ \frac{1}{T_T^{\alpha-1}} - \frac{1}{T_f^{\alpha-1}} \right\}$$

$$\lim_{T_f \to \infty} t_T = \frac{1}{k(\alpha-1} \frac{1}{T_T^{\alpha-1}}$$

b. $\alpha = 1$

$$t_T = \frac{1}{k}\left(\ell n\, T_f - \ell n\, T_T \right)$$

$$\lim_{T_f \to \infty} t_T = \infty$$

c. $0 \leq \alpha < 1$

$$t_T = \frac{1}{k(1-\alpha)} \left(T_f^{1-\alpha} - T_T^{1-\alpha} \right)$$

d. $\alpha < 0$

$$t_T = \frac{1}{k(\beta+1)} \left(T_f^{\beta+1} - T_T^{\beta+1} \right)$$

$$\beta = - \alpha \, , \quad \beta > 0 \, .$$

These solutions, regarded as a function of T_f, give Fig 3.3 .

References

Batchelor, G. K. 1952, Proc.Roy.Soc. A213, 349-366.

Board, S. J., Farmer, C. L. and Poole, D. H. 1972, CEGB Report No. RD/8/N2423.

Brauer, F. E., Green, N. W. and Mesler, R. B. 1968, Nuc.Sci.Eng. 31, 551-554.

Buchanan, D. J. 1973a, Submitted to J. Phys. D.

Buchanan, D. J. 1973b, J. Phys. D. 6, No 15.

Buchanan, D. J. 1973c, High Temperatures-High Pressures, (in the press).

Buchanan, D. J. and Dullforce, T. A. 1973, Nature 245, 32-34.

Chichelli, M. T. and Bonilla, C. F., 1945, Trans. Am. Inst. Chem.Engrs. 41, 755-787.

Christiansen, J. P. 1970, Culham Laboratory Report CLM-R106.

Christiansen, J. P. and Reynolds, J. A. 1971, unpublished work performed at Culham Laboratory.

Cole, R. H. 1965, Underwater Explosions, p 22, Dover Publications.

Döring, W. 1937, Z.physik. Chem. B36, 371-386.

Dullforce, T. A. and Buchanan, D. J. 1973, to be submitted for publication in J.Phys.D.

Enger, T., Hartman, D. E. and Seymour, E. V. 1972, Paper presented at the Cryogenic Engineering Conference, NBS, Boulder, Colorado.

Farahat, M. M. K., 1972, Argonne National Laboratory, Reactor Analysis and Safety Division Report, ANL-7909.

Farber, E. A. and Scorah, R. L., 1948, Trans. Am. Soc. Mech. Engrs. 70, 369-384.

Groenveld, P. 1972, J. Heat Transfer Trans. ASME. C94, 236-238.

Hesse, G., 1973, Int. J. Heat Mass Transfer, 16, 1611-1627.

Hinze, J. O. 1948, App. Sci. Res. A1, 273-288.

Katz, D. L. and Sliepcevich, C. M. 1971, Hydrocarb. Proc. Petrol. Refin. Nov. 240-244.

Katz, D. L. 1972, Chem. Eng. Prog. 68, 68-69.

Peckover, R. S. 1971, unpublished work performed at Culham Laboratory.

Plesset, M. S. and Chapman, R. B. 1971, J. Fluid Mech. 47, 283-290.

Potter, R. and Jakeman, D. 1972a, Paper No. 9 at the CREST Meeting on Sodium-Fuel Interaction in Fast Reactor Safety, Grenoble, January 1972.

Potter, R. and Jakeman, D. 1972b, Paper presented to the International Conference on Engineering of Fast Reactors for Safe and Reliable Operation, Karlsruhe, October 1972.

Roberts, K. V. 1972, Paper No. 20 at the CREST Meeting on Sodium-Fuel Interaction in Fast Reactor Safety, Grenoble, January 1972.

Rodebush, W. H. 1952, Ind. Eng. Chem. 44, 1289-1291.

Swift, D., 1965, Argonne National Laboratory, Chemical Engineering Division Semi-Annual Report, ANL-7125, p 192.

Taylor, G. I. 1963, Scientific Papers Vol. 3 (Ed. G. Batchelor), paper 32, CUP.

Walford, F. J., 1969, Int. J. Heat Mass Transfer, 12, 1621-1625.

Witte, L. C., Cox, J. E. and Bouvier, J. E. 1970, J. Metals 22, 39-44.

Yang, K. 1973, Nature, 243, 221-22.

Cycle No. i	Energy of bubble E (i) J	Final radius of bubble R_m (i) m	Elapsed time T (i) secs	Mass of coolant used kg	Peak pressure at r $P_i(r)-P_o$ bars	Impulse at r $I_i(r)$ N/m^2s
1	1.261×10^{-4}	6.673×10^{-4}	2.687×10^{-3}	2.176×10^{-11}	3.339	5.354×10^{-3}
2	3.747×10^{-2}	4.453×10^{-3}	5.813×10^{-3}	6.487×10^{-9}	22.28	2.382×10^{-1}
3	1.113×10^{1}	2.971×10^{-2}	1.197×10^{-2}	1.927×10^{-6}	148.7	1.060×10^{1}
4	3.307×10^{3}	1.983×10^{-1}	3.898×10^{-2}	5.726×10^{-4}	992.1	4.729×10^{2}
5	9.827×10^{5}	1.323×10^{o}	2.094×10^{-1}	1.701×10^{-1}	6620.	2.104×10^{4}

Table 3.1 Variation of energy, time, pressure and impulse with cycle number (P_o = 1 bar, $r_1 = 10^6$ $Jm^{-2}s^{-1}$, $r_2 = 10^3$ $Jm^{-2}s^{-1}K^{-1}$, $s_m = 3 \times 10^{-7}$ m).

$r_1 Jm^{-2}s^{-1}K^{-1}$	T (4) secs	E (4) J
10^6	3.898×10^{-2}	3.307×10^{3}
10^7	2.850×10^{-2}	3.307×10^{3}
10^8	1.269×10^{-2}	8.169×10^{1}
10^9	1.467×10^{-3}	3.390×10^{-2}

Table 3.2 Variation of r_1 (P_o = 1 bar, $r_2 = 10^3\ Jm^{-2}s^{-1}K^{-1}$, $s_m = 3 \times 10^{-7}$ m)

$r_2 Jm^{-2}s^{-1}K^{-1}$	T (4) secs	E (4) J
10^1	3.163×10^{-2}	3.307×10^{3}
10^2	3.181×10^{-2}	3.307×10^{3}
10^3	3.898×10^{-2}	3.307×10^{3}

Table 3.3 Variation of r_2 (P_o = 1 bar, $r_1 = 10^6\ Jm^{-2}s^{-1}$, $s_m = 3 \times 10^{-7}$ m)

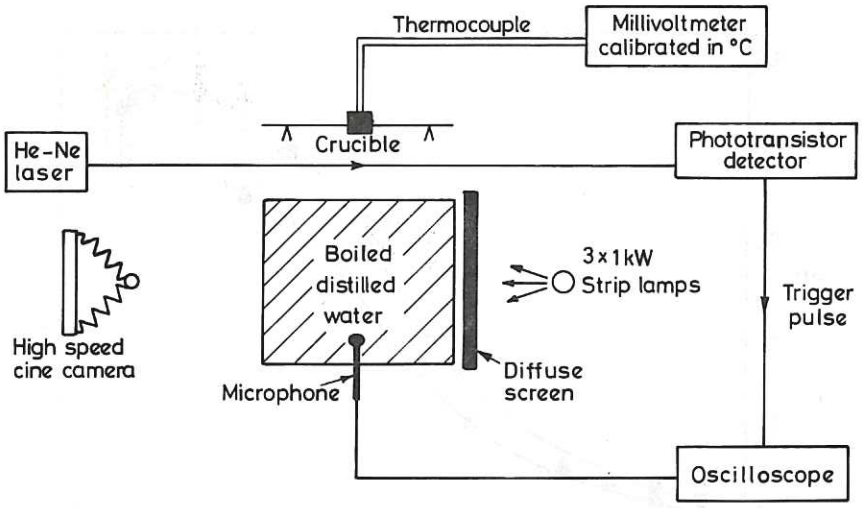

Fig.2.1 Experimental arrangement.

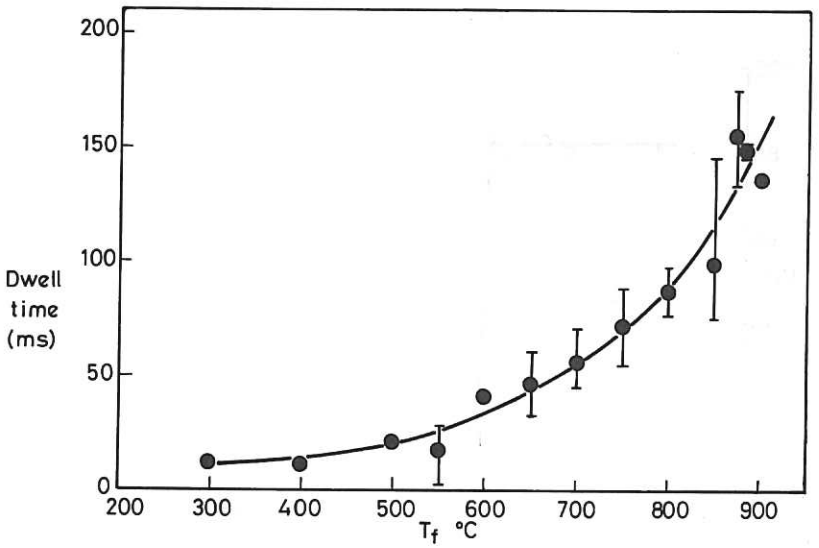

Fig.2.2 Measured dwell times for molten tin dropped into boiled distilled water at 34°C. Each point represents a single experiment, except where a vertical bar is included. In these latter cases the point is the average of several measurements and the bars represent the range found.

CLM-P362

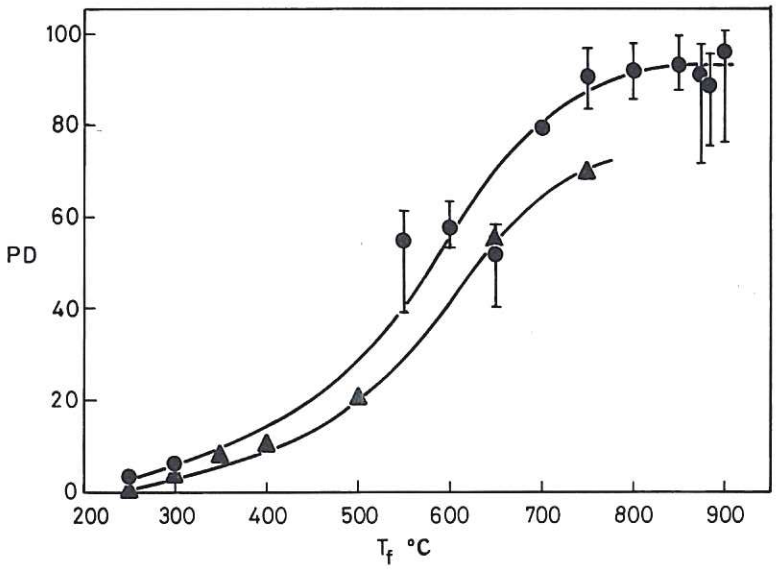

Fig.2.3 PD of dispersed tin as a function of T_f.
● Present experiments: boiled distilled water at 34°C.
▲ McCracken's experiments: tap water at 12°C.
The bars represent the range of values found.

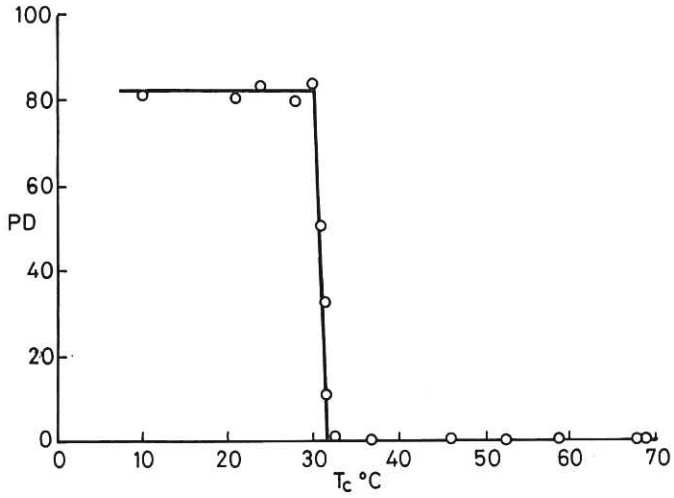

Fig.2.4 PD of dispersed metal (indium T_f = 800°C) as a function of T_c showing the coolant threshold temperature.

CLM-P362

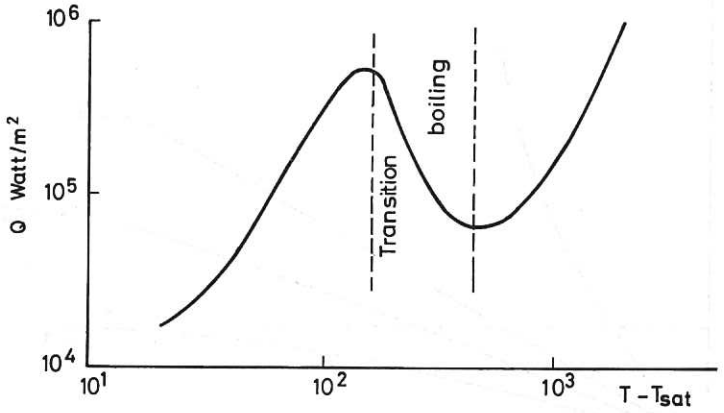

Fig.3.1 A typical boiling curve: Q is the heat flux and $T-T_{sat}$ the difference between the heating surface temperature and the saturation temperature. The transition boiling regime is shown.

CLM-P362

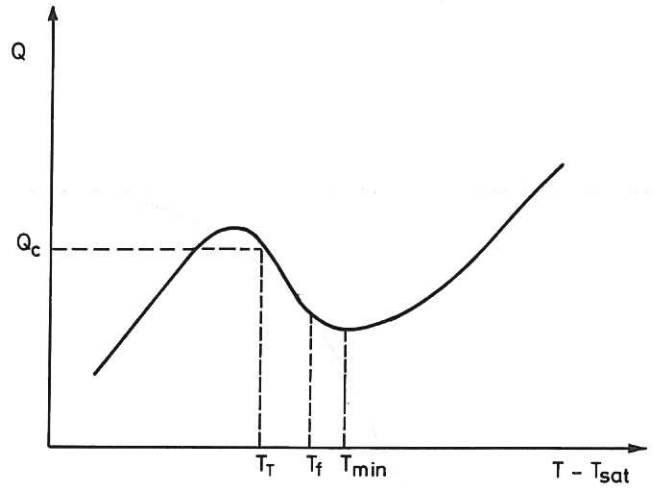

Fig.3.2 Boiling curve showing the location of Q_c. T is the fuel surface temperature and T_{min} corresponds to the trough.

CLM-P362

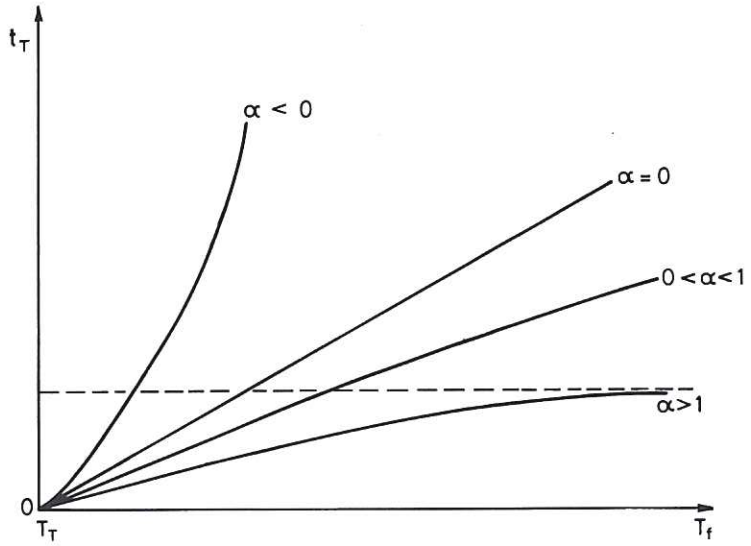

Fig.3.3 The time t_T to cool from T_f to T_T for various values of α. The dotted line represents the limit for t_T in the cases $\alpha > 1$.

CLM-P362

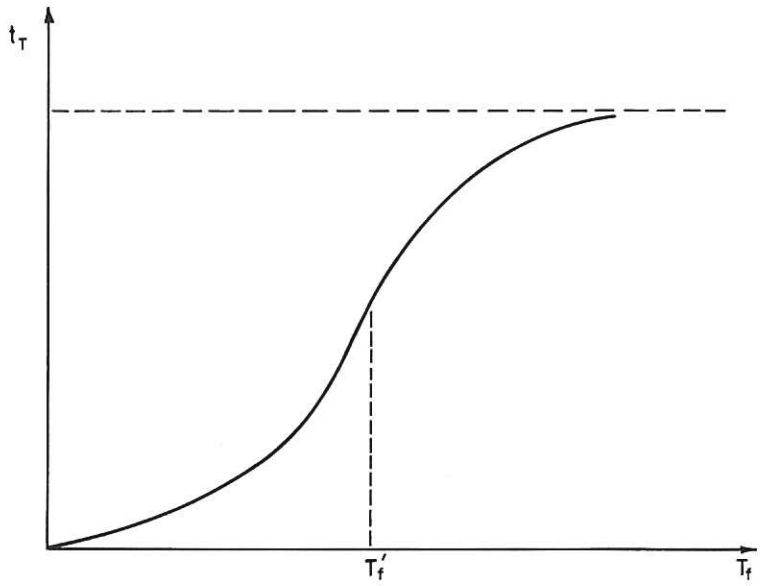

Fig.3.4 Qualitatively predicted dwell time curve. T_f' represents the limit of present experiments.

CLM-P362

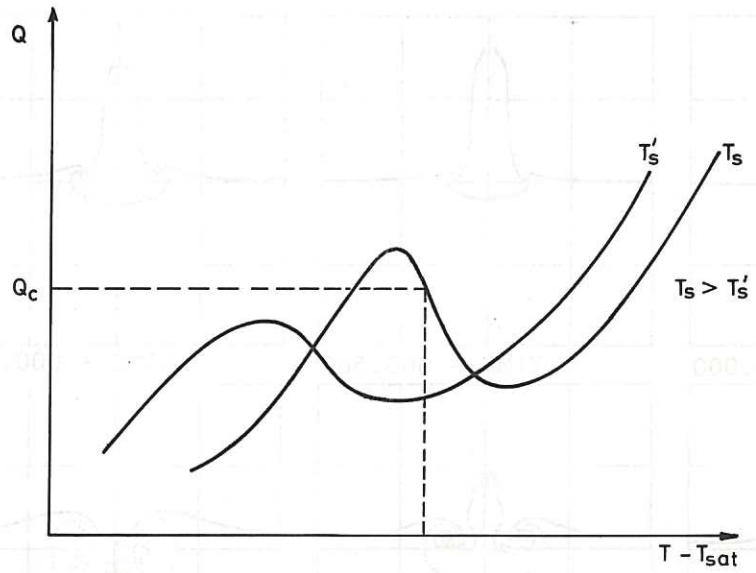

Fig.3.5 First explanation of the coolant cut-off temperature: Q_c is not attained. T_s and T_s' are two different subcoolings.

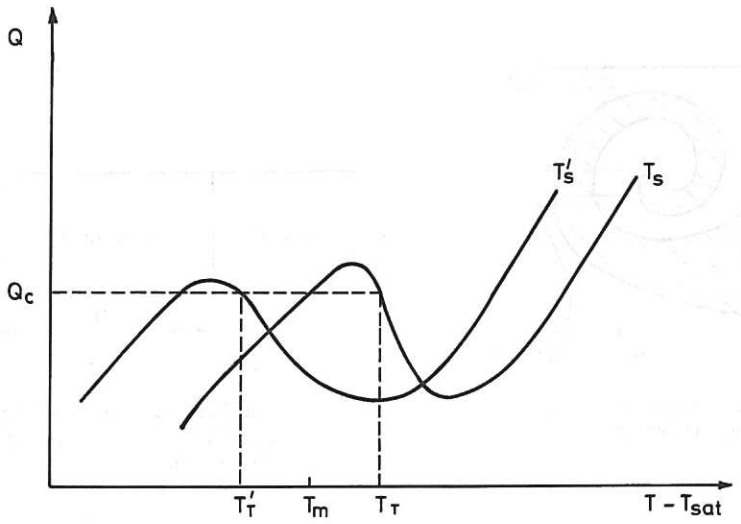

Fig.3.6 Second explanation of the coolant cut-off temperature: where Q_c is attained the fuel has solidified. T_s and T_s' are two different subcoolings and T_m is the melting temperature of the fuel. ($T_s > T_s'$).

CLM-P362

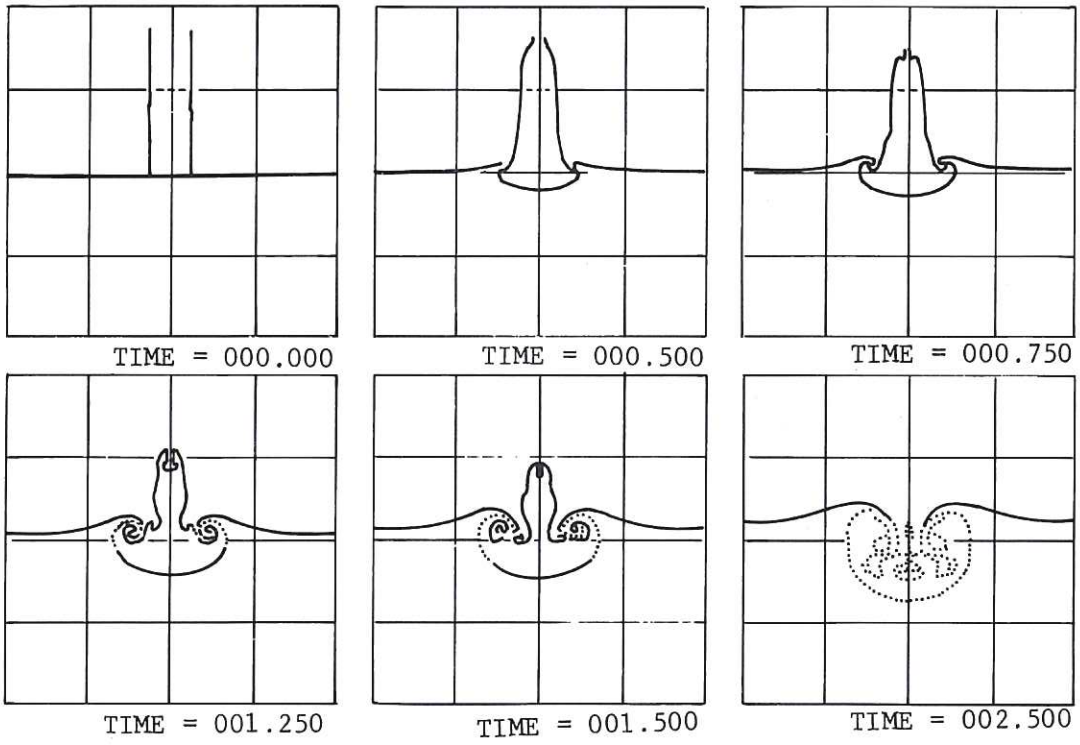

Fig.3.7 Computer simulation of penetration of a liquid by a liquid jet.

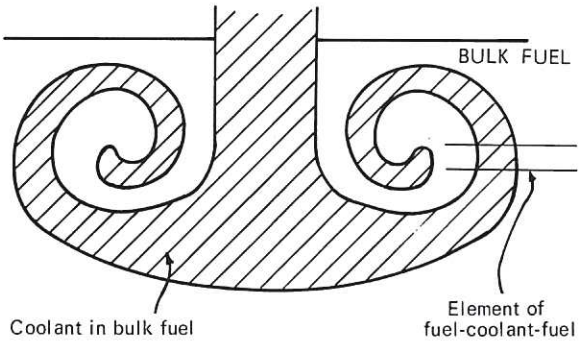

Fig.3.8 Schematic cross-section of a jet of coolant sometime after penetration.

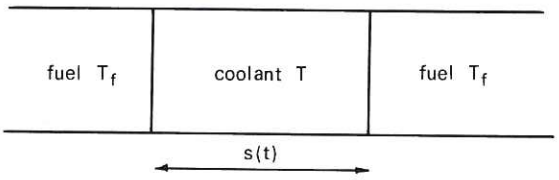

Fig.3.9 Element of fuel-coolant-fuel in which heat transfer occurs one-dimensionally.

CLM-P362

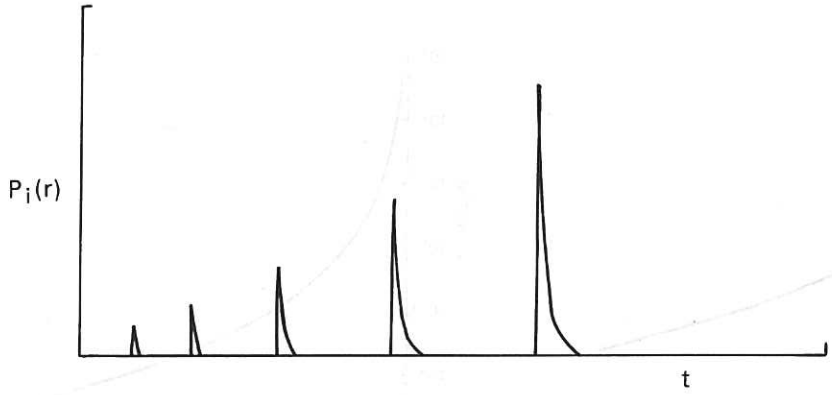

Fig.3.10 Pressure at the point r as a function of time.

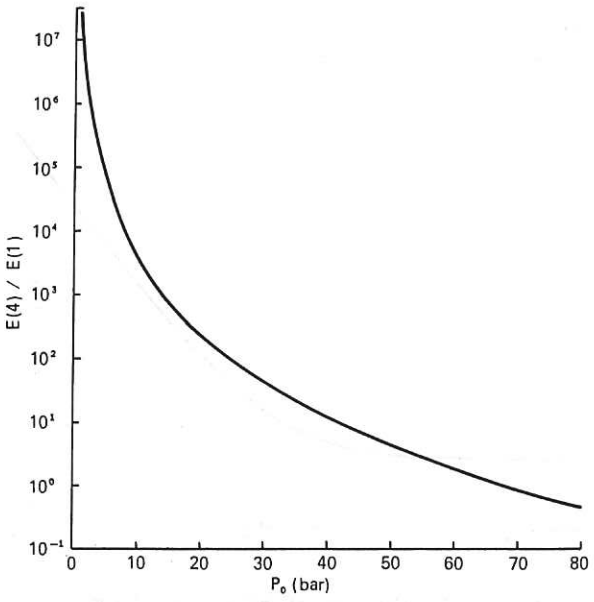

Fig.3.11 The effect of external pressure on the energy released: E(4)/E(1) v P_o. (For Figs.3.11-3.15, $r_1 = 10^6$ J $m^{-2}s^{-1}$, $r_2 = 10^3$ J $m^{-2}s^{-1}K^{-1}$ sm = 3×10^{-7} m).

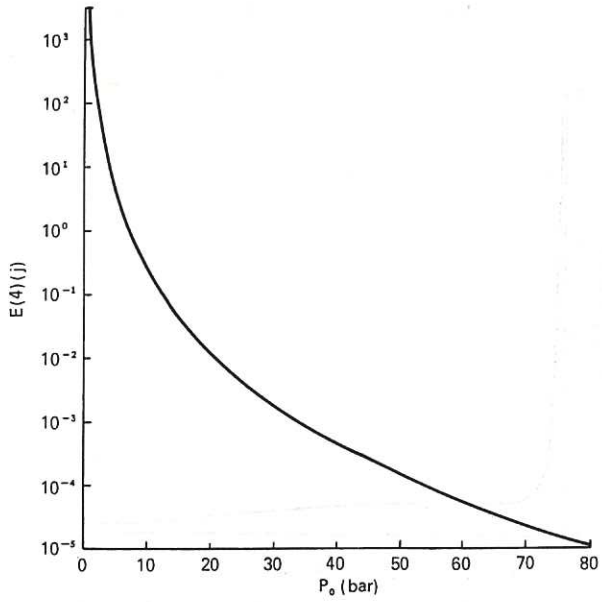

Fig.3.12 The effect of external pressure on energy released: E(4) v P_o.

CLM-P362

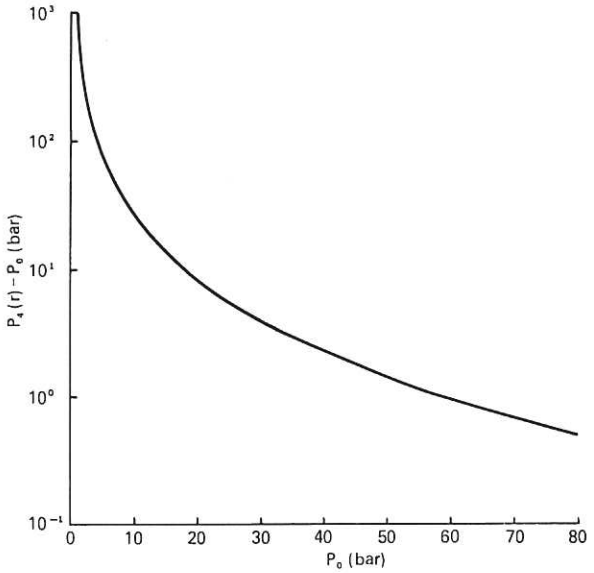

Fig.3.13 The effect of external pressure on the pressure measured at r: $P_4(r) - P_o$ v P_o.

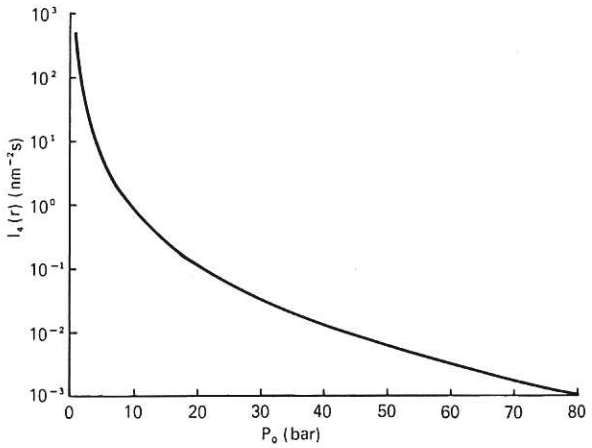

Fig.3.14 The effect of external pressure on the impulse felt at r: $I_4(r)$ v P_o.

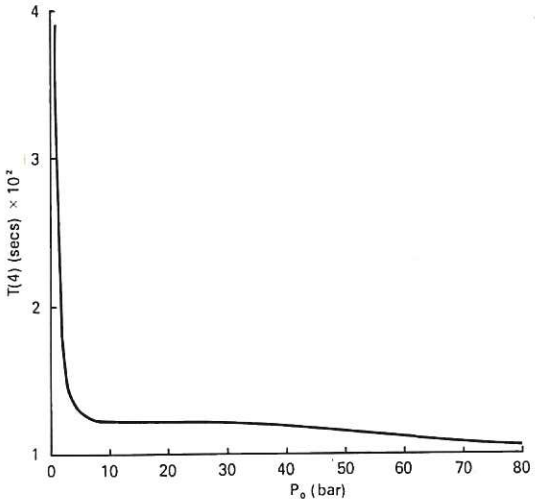

Fig.3.15 The effect of external pressure on the elapsed time: T(4) v P_o.

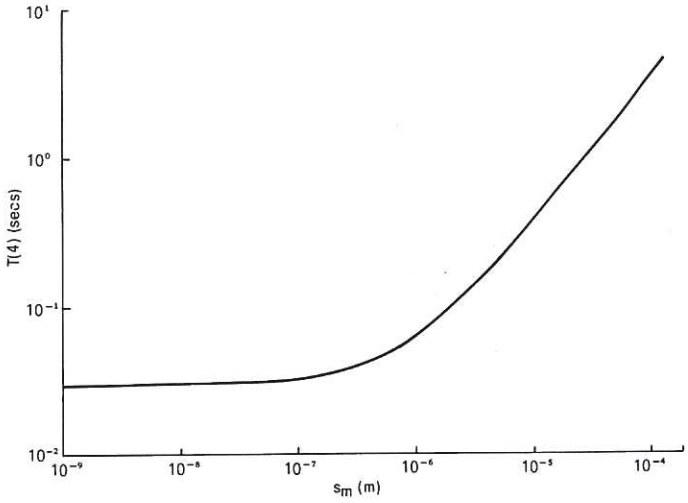

Fig.3.16 The effect of the minimum particle size on the elapsed time: T(4) v s_m.

CLM-P362

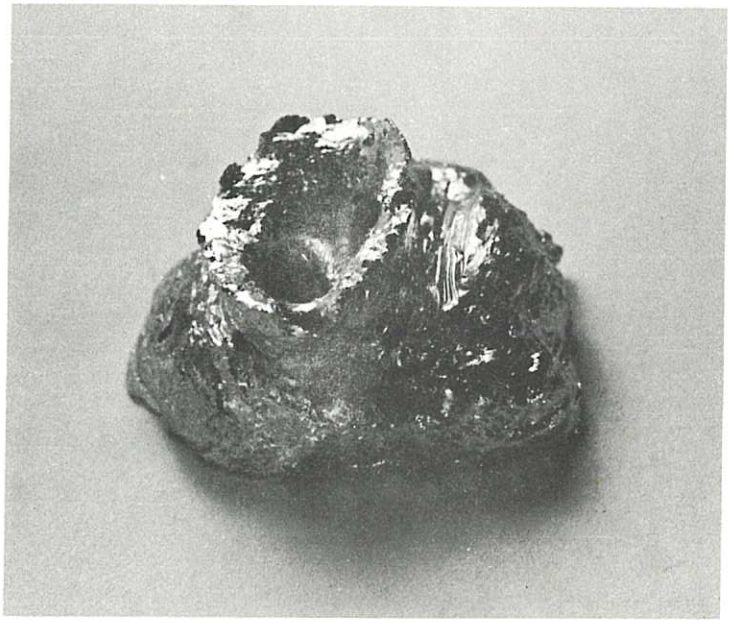

Plate 1: Photographic evidence showing explosions from within lumps of fuel.

Plate 2: Photographic evidence of jet penetration.

CLM-P362